Interferometric phase microscopy for label-free morphological evaluation of sperm cells

Miki Haifler, M.D.,[a,b] Pinhas Girshovitz, M.Sc.,[a] Gili Band, Ph.D.,[c] Gili Dardikman,[a] Igal Madjar, M.D.,[c] and Natan T. Shaked, Ph.D.[a]

[a] Department of Biomedical Engineering, Faculty of Engineering, Tel-Aviv University, Ramat Aviv; and [b] Department of Urology and [c] Male Fertility Clinic, Chaim Sheba Medical Center, Ramat Gan, Israel

Objective: To compare label-free interferometric phase microscopy (IPM) to label-free and label-based bright-field microscopy (BFM) in evaluating sperm cell morphology. This comparison helps in evaluating the potential of IPM for clinical sperm analysis without staining.
Design: Comparison of imaging modalities.
Setting: University laboratory.
Patient(s): Sperm samples were obtained from healthy sperm donors.
Intervention(s): We evaluated 350 sperm cells, using portable IPM and BFM, according to World Health Organization (WHO) criteria. The parameters evaluated were length and width of the sperm head and midpiece; size and width of the acrosome; head, midpiece, and tail configuration; and general normality of the cell.
Main Outcome Measure(s): Continuous variables were compared using the Student's *t* test. Categorical variables were compared with the χ^2 test of independence. Sensitivity and specificity of IPM and label-free BFM were calculated and compared with label-based BFM.
Result(s): No statistical differences were found between IPM and label-based BFM in the WHO criteria. In contrast, IPM measurements of head and midpiece width and acrosome area were different from those of label-free BFM. Sensitivity and specificity of IPM were higher than those of label-free BFM for the WHO criteria.
Conclusion(s): Label-free IPM can identify sperm cell abnormalities, with an excellent correlation with label-based BFM, and with higher accuracy compared with label-free BFM. Further prospective clinical trials are required to enable IPM as part of clinical sperm selection procedures. (Fertil Steril® 2015;104: 43–7. ©2015 by American Society for Reproductive Medicine.)
Key Words: Interferometry, phase microscopy, male fertility, sperm analysis

Discuss: You can discuss this article with its authors and with other ASRM members at http://fertstertforum.com/haiflerm-interferometric-phase-microscopy-sperm/

Use your smartphone to scan this QR code and connect to the discussion forum for this article now.*

* Download a free QR code scanner by searching for "QR scanner" in your smartphone's app store or app marketplace.

After the introduction of in vitro fertilization (IVF) extensive research was conducted to identify the morphologies of the oocyte and fetus as a prognostic tool (1). Fewer studies were conducted on the ability of sperm cell morphology to predict the success rates of natural fertilization, intrauterine insemination, IVF, and IVF with intracytoplasmic sperm injection (ICSI) (2–4). Typically, sperm cells are imaged optically using bright-field microscopy (BFM) and chosen according to World Health Organization (WHO) guidelines (5). Recently, new methods were developed for identifying finer properties of sperm cells that are not shown with BFM (e.g., surface charge selection [6]). Most of these methods involve biochemical preparations that might change the viability of the cells and thus preclude their use in IVF.

Without staining, sperm cells are nearly transparent under BFM, because their optical properties differ only slightly from those of their surroundings, resulting in a weak image contrast. An internal contrast mechanism that can be used when imaging sperm cells is their refractive index. The light beam that passes through the sperm cells is delayed, because the cells have a slightly higher refractive index compared with their surroundings. Regular, intensity-based detectors are not fast enough to record this delay directly.

Phase imaging methods, on the other hand, use the optical interference phenomenon to record the delays in the

Received January 16, 2015; revised and accepted April 9, 2015; published online May 21, 2015.
M.H. has nothing to disclose. P.G. has been issued a patent on the TAU inteferometer. G.B. has nothing to disclose. G.D. has nothing to disclose. I.M. has nothing to disclose. N.T.S. has been issued a patent on the TAU interferometer; and has a patent pending on sperm imaging using IPM.
M.H. and P.G. should be considered similar in author order.
Supported by a grant from the Ela Kodesz Institute for Medical Engineering and Physical Sciences at Tel Aviv University.
Reprint requests: Natan T. Shaked, Ph.D., Department of Biomedical Engineering, Tel Aviv University, Ramat Aviv 69978, Israel (E-mail: nshaked@post.tau.ac.il).

Fertility and Sterility® Vol. 104, No. 1, July 2015 0015-0282/$36.00

http://dx.doi.org/10.1016/j.fertnstert.2015.04.013

passage of light through the sample, and they are able to create label-free contrast in the image. However, conventional phase-contrast imaging methods for sperm cells, such as Zernike's phase contrast (7), and Nomarski's differential interference contrast (DIC), which is the basis for the motile sperm organelle morphology examination (MSOME) technique (8), are not fully quantitative, because they do not create meaningful contrast on all points of the measured sperm. In addition, these techniques present significant imaging artifacts, especially near the cell edges, which may yield incorrect morphological assays.

Interferometric phase microscopy (IPM) (9) is a holographic imaging method, which allows for a fully quantitative measurement of the cell optical thickness (i.e., the product of the refractive index and the physical thickness) on all the sperm spatial points. This method requires a lower illumination power and presents high throughput because capturing is done in a single exposure and without scanning. Holographic imaging has been identified previously as a tool for sperm measurements (10, 11). However, until recently, most IPM setups were bulky, expensive, and hard to operate. Recently, we have developed a portable and easy-to-operate IPM module, which can be attached to existing clinical microscopes and provide label-free, quantitative contrast for cell samples (12, 13).

Sperm cell morphology is known to be an indicator of its fertilization potential (2–4). Therefore, improved noninvasive morphological assays for sperm cells are needed. These assays are expected to be especially important for cases in which cell labeling is not recommended. One specific example is IVF with ICSI for sperm cells of infertile males. In these cases, quantitative morphological imaging might be the best predictor for choosing the most suitable sperm cell for injection into the oocyte.

To date, however, no research has compared label-free IPM with BFM, using the WHO criteria. The aim of the present study is to compare IPM with BFM, in sperm cell evaluation, to examine the potential validity of this method as a clinical tool for sperm analysis.

MATERIALS AND METHODS

Sample Preparation and Imaging

After institutional ethics committee approval, normal and pathologic sperm samples were received from the male fertility clinic at Chaim Sheba Medical Center. After the samples were collected, using methods in accordance with the WHO manual (5), a drop of 5–10 μl of fresh semen was smeared onto a clean microscope slide (24 × 50 mm) and left to dry for 5 minutes. Before the sample was imaged, it was fixed in 98% ethanol for 10 minutes.

Morphological evaluation was performed on the same sperm cells, using IPM (see next section) and BFM with an inverted microscope (Axio Observer D1, Zeiss). To find the same sperm in different imaging modalities, each slide was painted with a 2 × 2 point grid. After the samples were imaged without labeling (in label-free BFM and IPM), they were stained with Quick Stain (Biological Industries), left to dry for 15 minutes, and imaged again in label-based BFM. All measurements were performed by one of the investigators, who is a trained urologist, accompanied by the biomedical engineer investigator, who built the optical systems, to allow optimal imaging results.

Interferometric Phase Microscopy System

The proposed IPM optical system is depicted in Supplemental Figure 1 (available online). Briefly, the system is comprised of our previously developed portable interferometric module (τ interferometric) (13), connected at the exit of a regular inverted microscope.

In this system, a partially monochromatic light source (6.2-nm–wavelength bandwidth) illuminates an existing inverted microscope for sperm analysis. The τ portable interferometric module is a small box, connected at the port of the microscope output (where the camera is usually positioned), and projects an interference pattern on the digital camera, allowing quantitative phase acquisition. This interference is created by projecting two beams onto the camera with a small angle between them: a sample beam, which is the regular magnified image of the sperm sample; and a reference beam, which does not contain the sample information. The interference pattern is acquired by a regular digital camera in a single exposure, and can be digitally processed, by a conventional computer in real time, to the optical thickness map of the sperm, allowing a fully quantitative contrast image of the sperm sample, without any labeling.

Unlike previous IPM setups that require custom-built microscopes, expensive equipment, and difficult alignment, our setup is robust, portable to existing clinical microscopes, and easy to align. A detailed description of the setup and the following digital image analysis is given in Supplemental Appendix 1 (available online).

Statistical Analysis

The following variables were collected using IPM, label-free BFM, and labeled-based BFM: length and width of sperm head, number and relative size of head vacuoles, width and relative size of the acrosome, and length and width of the midpiece. Furthermore, qualitative assessment of the form of the midpiece, length and form of the tail, and general form of the sperm cell were also gathered.

Continuous variables were presented as mean (±SD) and evaluated by the paired Student's t test and the Wilcoxon signed rank test, as applicable. Categorical variables were presented as percentages and evaluated with the χ^2 test of independence and McNemar's test, as needed. In addition, sensitivity and specificity of IPM and label-free BFM were calculated, and compared with label-based BFM. The number of sperm cells needed for evaluation was chosen so as to be able to identify a 10% difference in any of the continuous variables at $P<.05$ and at a power of 80%. Statistical analysis was performed with SPSS, version 21 (IBM).

RESULTS

Figure 1A and B show a typical interferogram obtained using the IPM system. The bending of the interference fringes over

FIGURE 1

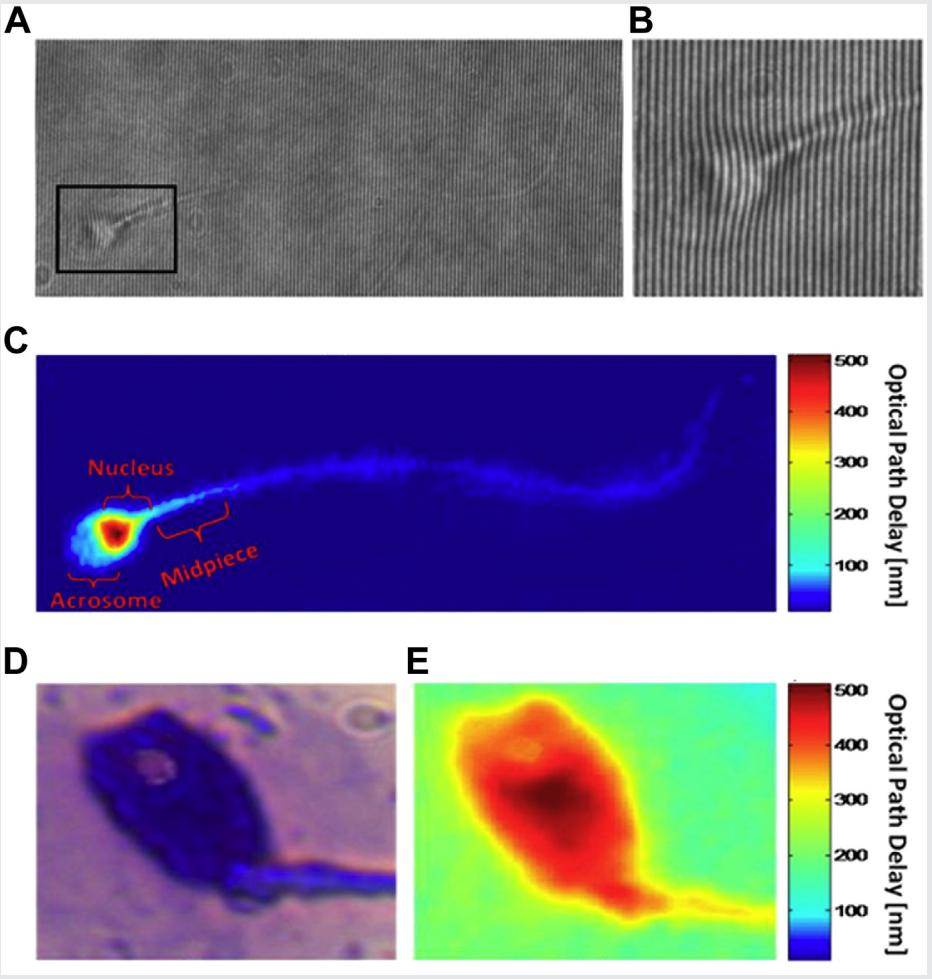

(**A**) An interferogram obtained using IPM. As in label-free BFM, the sample is barely seen. However, the OPD information is encoded into the bending of the interference fringes, as can be seen from the enlarged region of interest in (**B**). (**C**) The OPD map of the same sperm cell, as digitally calculated from the interferogram shown in (**A**). All the main morphological features of the cell are discernable. (**D**, **E**) Imaging of a sperm cell with an acrosomal vacuole, using (**D**) label-based BFM, and (**E**) label-free IPM. The vacuole is clearly seen as a defect in the OPD map of the IPM image. BFM = bright-field microscopy; IPM = interferometric phase microscopy; OPD = optical path delay.

Haifler. Label-free IPM for sperm cell evaluation. Fertil Steril 2015.

the sperm cells, which are clearly seen, encodes the sperm thickness information. The reconstructed optical path delay (OPD) or optical thickness map of the sample (product of physical thickness and refractive index) is seen in Figure 1C. The colors represent the OPD values on the map. As can be seen in Figure 1, with use of IPM, the morphological details of the sperm sample can be visualized and analyzed without staining. An example of a head vacuole imaged by label-based BFM and by label-free IPM is presented in Figure 1D and E, respectively.

We evaluated 350 sperms cells, from 6 healthy and 2 pathologic sperm cell samples, according to the WHO criteria. In the label-based BFM measurements, 47.4% of the cells were abnormal looking. Head, midpiece, and tail defects were detected in 29.3%, 15.5%, and 22.4% of the cells, respectively. The average values of the continuous variables are presented in Table 1.

No statistically significant difference was identified in the continuous variables evaluated with IPM and label-based BFM. In contrast, head width, acrosome area, and midpiece width were statistically significantly different for IPM vs. label-free BFM. According to the analysis presented in Table 2, the categorical variables evaluated using IPM were dependent on the variables evaluated using label-based BFM. In contrast, the variables evaluated using label-free BFM were statistically independent of those found using label-based BFM.

The results of the sensitivity analysis of IPM and label-free BFM, compared with label-based BFM, are presented in Table 3. Sperm-head vacuoles were identified in 15 (4.2%), 24 (6.8%), and 5 (1.4%), using IPM, label-based BFM, and label-free BFM, respectively. All the vacuoles that were not identified with IPM were single and <5% of the sperm cell heads. However, 50% of the vacuoles that were missed by label-free BFM were identified using IPM.

TABLE 1

Descriptive statistics of the continuous variables with label-free IPM, label-based BFM, and label-free BFM.

Modality	Head length (μm)	Head width (μm)	Acrosome area (%)	Acrosome width (μm)	Midpiece width (μm)	Midpiece length (μm)	Size of largest vacuole (%)
IPM	4.99 ± 0.86	3.88 ± 0.78	35.5 ± 11.5	2.52 ± 0.66	1.14 ± 0.65	4.22 ± 1.42	12.7 ± 7.5
Label-based BFM	4.97 ± 0.66	3.79 ± 0.6	36.2 ± 12.4	2.62 ± 0.65	1.2 ± 0.84	4.3 ± 0.72	10 ± 5
P value	.775	.244	.449	.168	.506	.563	.082
Label-free BFM	4.97 ± 0.64	3.6 ± 0.59	54.6 ± 17.5	2.51 ± 0.52	0.83 ± 0.37	4.38 ± 0.74	13 ± 4.4
P value	.577	< .001	< .001	.21	< .001	.5	.9

Note: Values are given with ±SD.

Haifler. Label-free IPM for sperm cell evaluation. Fertil Steril 2015.

DISCUSSION

Infertility is a common condition that affects 15% of couples who are trying to have children. Few treatment options were available, until IVF was introduced in the late 1970s. After its introduction, the fact that patients with abnormal semen analysis had a lower probability of successful pregnancies using IVF soon became obvious (14). The next important step was achieved in 1992, when the first successful ICSI was reported (15). In the ICSI process, the best-looking motile sperm is chosen and then injected into an oocyte that has been retrieved from the female partner. Other than adoption, ICSI is the only treatment option for severe male factor infertility (e.g., oligo-terato-asthenospermia). However, the success rate of ICSI (measured by clinical pregnancy or live birth rate) is still very low (16).

Ideally, the sperm that is chosen for ICSI should have the highest chance of successful fertilization and subsequent embryo growth. To achieve this goal, advanced sperm-selection techniques were developed, such as electrophoretic isolation (6). However, accumulating evidence showed little or no improvement in fertility outcomes (17).

The label-free optical method for sperm analysis known as MSOME (8) utilizes DIC microscopy, which is based on splitting the illumination light beam into two parts, which are spatially displaced at the sample plane, and recombined before observation. The interference of the two parts is sensitive to their OPD gradient, creating an edge-shadowing effect (18). However, DIC microscopy is not fully quantitative, because it does not provide contrast on the entire cell image, only edge enhancement. Second, a shading effect, which is dependent on the two-beam shear, is created. For these reasons, the resulting image cannot be interpreted as a meaningful physical measurement of the cell, such as cell thickness, on all cell spatial points. Furthermore, the shading effect might obscure important morphological features (19). Third, DIC requires dedicated equipment, which is not widely available in fertility clinics. Initially, MSOME was believed to improve reproductive outcomes (8). However, a recent report claims that MSOME has not improved the fertility success rate to date (14).

In recent years, several initial studies have demonstrated use of IPM (also called digital holographic microscopy) for sperm imaging. Coppola et al. (10) used IPM to evaluate sperm, mainly based on the presence or absence of vacuoles. Because vacuoles form early in spermatogenesis, they may reflect defects in sperm content, and therefore, these cells should be avoided in ICSI. Crha et al. (20) used IPM to compare normal and pathological sperm samples with IPM. These authors showed that abnormal sperm heads have lower maximal OPD compared with normal samples. Sperm movement characterization was also assessed using IPM, by Di Caprio et al. (11). However, so far, no research has compared IPM and BFM in relation to the WHO criteria.

We indeed found a statistically significant difference in head width, acrosome area, and midpiece width between IPM and label-based BFM. No difference was identified in head length, acrosome width, midpiece length, or size of the largest vacuole between IPM and label-based BFM. In contrast, no statistically significant difference was found in these parameters between label-based BFM and label-free BFM. These results suggest that label-free IPM can provide quantitative information on sperm cell morphology that is comparable to label-based BFM and more accurate than label-free BFM.

Furthermore, the binary (normal/abnormal) system, recommended by the WHO, was examined on the categorical parameters (e.g., head and midpiece form, overall evaluation)

TABLE 2

Prevalence of sperm defects diagnosed by label-free IPM, label-based BFM, and label-free BFM.

Modality	Head configuration	Midpiece form	Tail form	Tail length	Global evaluation
Label-based BFM	29.3	15.5	22.4	22.4	47.4
IPM	30.3	14.7	19.8	16.4	45.7
P value	.032	< .001	< .001	< .001	< .001
Label-free BFM	20.7	11.2	18.1	24.1	48.3
P value	.5	.815	.86	.058	.098

Note: Values are percentages, unless otherwise indicated.

Haifler. Label-free IPM for sperm cell evaluation. Fertil Steril 2015.

TABLE 3

Sensitivity analysis of IPM and label-free BFM.

Measure and modality	Sensitivity	Specificity
Head form		
IPM	45	75
Label-free BFM	30.8	78.5
Midpiece form		
IPM	76.5	96.7
Label-free BFM	25	87.5
Tail form		
IPM	84	97.5
Label-free BFM	20	79
Tail length		
IPM	68	97.4
Label-free BFM	45	73.5
Global evaluation		
IPM	82	85
Label-free BFM	60	43.5

Note: Values are percentages. Both the sensitivity and specificity of IPM were higher than those of label-free BFM.

Haifler. Label-free IPM for sperm cell evaluation. Fertil Steril 2015.

(5). Label-based BFM measurements were dependent with these of IPM, and independent with these of label-free BFM. Given that we considered label-based BFM to be the gold standard in this study, these results bolster our hypothesis that IPM is superior to label-free BFM in evaluating sperm cell morphology. Finally, by performing sensitivity analysis on label-free BFM and IPM for the categorical variables, we found that IPM is more sensitive to sperm cell defects than is label-free BFM, and can thereby better differentiate normal-looking from abnormal-looking cells.

Typical IPM is too complicated, bulky, and expensive to be implemented in fertility clinics. In this regard, our IPM module provides a considerable advantage, because it is portable, easy to operate, and inexpensive. In addition, IPM potentially can provide further information of interest in regard to the fertilizing potential of the sperm cell, such as cell thickness, dry mass, and volume.

Our study had several limitations. First, we examined fixed cells and not live motile cells, because we wanted to compare the exact same sperm cells using several imaging modalities. However, because IPM requires a single camera exposure, it can be used additionally for examining sperm motility (21). Second, this study is a pilot of the feasibility of IPM as a tool for sperm analysis. Most certainly, further prospective studies are needed to show that IPM improves pregnancy or birth rates after ICSI. Third, we have not fully compared IPM with any of the other advanced methods for sperm cell selection, such as MSOME, because we believe that comparing IPM to the gold-standard, label-based BFM is the first step.

In conclusion, portable IPM is a novel and affordable method for observing and analyzing sperm cell characteristics without the need for sample preparation or labeling. We found our label-free method to be equivalent to label-based BFM, and superior to the commonly used label-free BFM, in assessing morphological parameters of sperm samples. Further prospective clinical trials are required to evaluate label-free IPM as a clinical tool for sperm analysis, and the outcomes of using it for fertility procedures.

REFERENCES

1. Steptoe PC, Edwards RG. Birth after the reimplantation of a human embryo. Lancet 1978;2:366.
2. Kruger TF, Acosta AA, Simmons KF, Swanson RJ, Matta JF, Oehninger S. Predictive value of abnormal sperm morphology in in vitro fertilization. Fertil Steril 1988;49:112–7.
3. Bartoov B, Eltes F, Pansky M, Lederman H, Caspi E, Soffer Y. Estimating fertility potential via semen analysis data. Hum Reprod 1993;8:65–70.
4. Berkovitz A, Eltes F, Soffer Y, Zabludovsky N, Beyth Y, Farhi J, et al. ART success and in vivo sperm cell selection depend on the ultramorphological status of spermatozoa. Andrologia 1999;31:1–8.
5. World Health Organization. WHO laboratory manual for the examination and processing of human sperm. Available at: http://www.who.int/reproductivehealth/publications/infertility/9789241547789/en. Last accessed May 10, 2015.
6. Ainsworth C, Nixon B, Aitken R. Development of a novel electrophoretic system for the isolation of human spermatozoa. Hum Reprod 2005;20:2261–70.
7. Zernike F. How I discovered phase contrast. Science 1955;121:345–9.
8. Bartoov B, Berkovitz A, Eltes F, Kogosowski A, Menezo Y, Barak Y. Real-time fine morphology of motile human sperm cells is associated with IVF-ICSI outcome. J Androl 2002;23:1–8.
9. Girshovitz P, Shaked NT. Generalized cell morphological parameters based on interferometric phase microscopy and their application to cell life cycle characterization. Biomed Opt Express 2012;3:1757–73.
10. Coppola G, Di Caprio G, Wilding M, Ferraro P, Esposito G, Di Matteo L, et al. Digital holographic microscopy for the evaluation of human sperm structure. Zygote 2014;22:446–54.
11. Di Caprio G, El Mallahi A, Ferraro P, Dale R, Coppola G, Dale B, et al. 4D tracking of clinical seminal samples for quantitative characterization of motility parameters. Biomed Opt Express 2014;5:690–700.
12. Shaked NT. Quantitative phase microscopy of biological samples using a portable interferometer. Opt Lett 2012;37:2016–8.
13. Girshovitz P, Shaked NT. Compact and portable low-coherence interferometer with off-axis geometry for quantitative phase microscopy and nanoscopy. Opt Express 2013;21:5701–14.
14. Teixeira DM, Barbosa MA, Ferriani RA, Navarro PA, Raine-Fenning N, Nastri CO, et al. Regular (ICSI) versus ultra-high magnification (IMSI) sperm selection for assisted reproduction. Cochrane Database Syst Rev 2013:CD010167.
15. Palermo G, Joris H, Devroey P, Van Steirteghem AC. Pregnancies after intracytoplasmic injection of single spermatozoon into an oocyte. Lancet 1992;340:17–8.
16. Jungheim ES, Ryan GL, Levens ED, Cunningham AF, Macones GA, Carson KR, et al. Embryo transfer practices in the United States: a survey of clinics registered with the Society for Assisted Reproductive Technology. Fertil Steril 2010;94:1432–6.
17. McDowell S, Kroon B, Ford E, Hook Y, Glujovsky D, Yazdani A. Advanced sperm selection techniques for assisted reproduction. Cochrane Database Syst Rev 2014:CD010461.
18. Murphy D. Differential interference contrast (DIC) microscopy and modulation contrast microscopy. In: Fundamentals of light microscopy and digital imaging. New York: Wiley-Liss; 2001:153–68.
19. Marquet P, Rappaz B, Magistretti PJ, Cuche E, Emery Y, Colomb T, et al. Digital holographic microscopy: a noninvasive contrast imaging technique allowing quantitative visualization of living cells with subwavelength axial accuracy. Opt Lett 2005;30:468–70.
20. Crha I, Zakova J, Huser M, Ventruba P, Lousova E, Pohanka M. Digital holographic microscopy in human sperm imaging. J Assist Reprod Genet 2011;28:725–9.
21. Girshovitz P, Shaked NT. Doubling the field of view in off-axis low-coherence interferometric imaging. Light: Sci Appl 2014;3:1–9.

SUPPLEMENTAL APPENDIX 1

DETAILED OPTICAL INTERFEROMETRIC SYSTEM DESCRIPTION AND MATHEMATICAL FORMULATION OF THE DIGITAL PROCESS

Supplemental Figure 1 (available online) presents the optical system, which is comprised of a light source, a conventional inverted microscope, a portable interferometric module, and a conventional digital camera, connected to a conventional personal computer. The light source used in the input of the inverted microscope is a supercontinuum fiber laser source (SC-400-4 Fianium), connected to a computer-controlled acousto-optical tunable filter (SC-AOTF, Fianium), emitting wavelengths of 532 $\pm$ 3.1 nm. Other, simpler light sources (e.g., laser diodes) can be used. The inverted microscope uses a single, 63×, 1.4 numerical aperture, oil immersion, infinity-corrected microscope objective, and a spherical tube lens with a 15-cm focal length. The digital camera in the output of the system was a monochromatic CMOS camera with 1280 × 1024 square pixels of 5.2 μm each (DCC1545M, Thorlabs).

The τ portable interferometric module is depicted at the bottom of Supplemental Figure 1, and is connected between the output port of the microscope and the digital camera. In this module, lenses L1 and L2 were chosen to be achromatic lenses with focal lengths of 100 mm and 150 mm, respectively. The image plane at the output of the inverted microscope is optically Fourier transformed by lens L1, and split by a beam splitter. One arm (sample beam, *dashed lines*) is reflected and shifted aside by a retro-reflector, and inverse Fourier transformed onto the camera plane by lens L2. The second arm (reference beam, *solid lines*) is spatially filtered by a pinhole that effectively erases the sample image spatial modulation, reflected by mirror M1, and inverse Fourier transformed onto the camera plane by lens L2. As a result of this configuration, the camera plane contains a superposition of two beams: the sample beam, containing the magnified image of the sperm sample, and a filtered reference beam that does not contain sample modulation (13 [in main text]).

The interference pattern captured by the camera is described mathematically as follows:

$$I = I_s + I_r + G_{+1} + G_{-1},$$

where I_s, I_r are the intensities of the sample and reference beams, and G_{+1}, G_{-1} are the cross-correlation functions (1). The optical path delay (OPD) of the sample can be digitally extracted using a conventional personal computer in real time (2). In this digital processing, the interferogram is two-dimensionally Fourier transformed in the computer. The cross-correlation function G_{+1} is separated from the other terms by a spatial band pass filter. The filtered cross-correlation function is centered and inverse Fourier transformed. The resulting complex function contains a phase argument (sample phase). The same process is performed for a sample-free interferogram (background phase). The background phase is subtracted from the sample phase to compensate for beam curvature and static aberrations. Finally, an unwrapping algorithm is applied, to remove 2π ambiguities from the phase map (3). The resulting unwrapped phase map $\varphi(m,n)$ is proportional to the OPD or optical thickness of the sample, as described by the following formula:

$$OPD(m,n) = \frac{\lambda}{2\pi}\varphi(m,n),$$

where m and n are the pixel coordinates, and λ is the light-source central wavelength (12 [in main text]). The OPD profiles of the sperm were extracted using Matlab R2013b software (MathWorks). After this, a graphic user interface was specifically designed, also using Matlab software, for collecting all the data from all imaging modalities, per each sperm image, into a database of variables, which eased the statistical analysis process.

REFERENCES

1. Saleh BAE, Teich MC. Statistical optics. In: Saleh BAE, editor. Fundamentals of photonics. Chichester: Wiley; 1991:403–42.
2. Girshovitz P, Shaked NT. Real-time quantitative phase reconstruction in off-axis digital holography using multiplexing. Opt Lett 2014;39:2262–5.
3. Ghiglia DC, Pritt MD. Two-dimensional phase unwrapping: theory, algorithms, and software. Chichester: Wiley; 1998.

SUPPLEMENTAL FIGURE 1

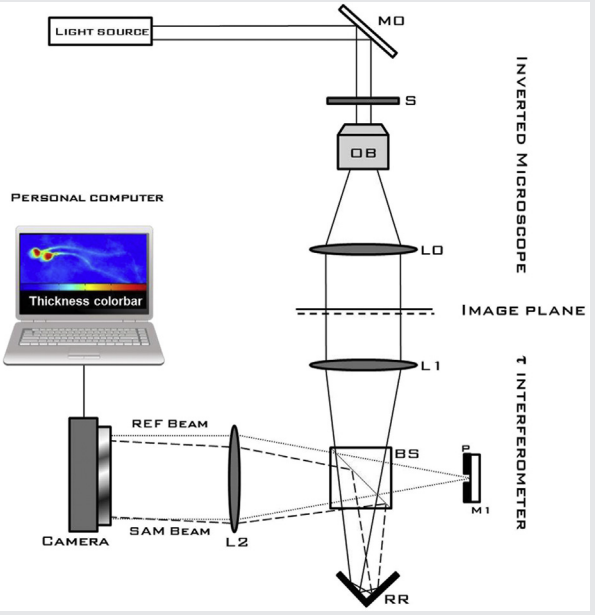

The proposed IPM system. See full description in Supplemental Appendix 1 (available online). BS = beam splitter; L0, L1, L2 = lenses; M0, M1 = mirrors; OB = objective lens; P = pinhole; REF = reference; RR = retro-reflector; S = sample; SAM = sample.

Haifler. Label-free IPM for sperm cell evaluation. Fertil Steril 2015.